Electromagnetic Launcher Notes

Note 1

26 December 2007

Some Electromagnetic Considerations for Design of Railgun Electromagnetic Projectile Launchers

Carl E. Baum
University of New Mexico
Department of Electrical and Computer Engineering
Albuquerque New Mexico 87131

Abstract

This paper explores some alternate design concepts for electromagnetic projectile launchers. This involves considerations of projectile geometry including the pusher plate, as well as the geometry of the current-carrying rails.

`

This work was sponsored in part by the Air Force Office of Scientific Research.

1. Introduction

An electromagnetic railgun is a device designed to launch a projectile at high speeds. It is powered by some electrical energy source (e.g., a capacitor bank) which provides a high urrent through a conductor on the projectile. For a sheet conductor, the force density (per unit area) or pressure is

$$\begin{aligned} &\vec{f} = \vec{J}_S \times \vec{B} \equiv \text{pressure } (N/m^2) \\ &\vec{J}_S \equiv \text{ sheet current density } (Am^{-1}) \\ &\vec{B} \equiv \text{ magnetic flux density (T)} \end{aligned} \tag{1.1}$$

in usual MKS units. The magnetic field is produced by the configuration of the currents in the railgun. The system is a low-impedance one allowing one to approximately neglect the electric-field forces. The magnetic forces can be quite large, thereby accelerating the projectile to hypervelocities.

There has been much work done on railguns. Here we cite only a few of the many papers on the subject [3-5]. The reader can find many more in the literature.

The purpose of the present paper is to suggest some design features which may give some alternate approaches to railgun design. These may have both advantages and disadvantages in practical railgun design.

2. Basic Railgun

As in Fig. 2.1, a basic railgun has two highly conducting rails which feed a current through a pusher plate (or even a plasma) giving a sheet current density $\vec{J}_s$ with

$$\int_{-y_0}^{y_0} \vec{J}_s \cdot \vec{1}_y \, dy \simeq I \tag{2.1}$$

Or roughly

$$2 y_0 | \vec{J}_s | \simeq I \tag{2.2}$$

Assuming a uniform sheet current density we have

$$\vec{J}_s \simeq J_{s_0} \vec{1}_x \tag{2.3}$$

Let us assume for the present calculations that the pusher plate is the only metal (highly conducting) on the projectile. Dielectrics can be chosen for the projectile so as not to significantly distort the magnetic field distribution.

Using basic symmetry considerations, then we can decompose the magnetic field into symmetric and antisymmetric parts [7] as indicated in Fig. 2.2. (Here we neglect the motion of the projectile.) The symmetric part has currents of I/2 on the rails, joining the pusher plate and giving it a current of *I*. This gives a sheet current density as in (2.2) provided care is taken to make the current density on the sheet uniform. In this case the boundary condition (jump discontinuity) at the sheet has

$$\vec{B}_{sy}^{(-)} = -\vec{B}_{sy}^{(+)} = \mu_0 \vec{H}_{sy}^{(-)} = \frac{\mu_0}{2} \vec{1}_y | \vec{J}_s | = \frac{\mu_0 I}{4 y_0} \vec{1}_y \tag{2.4}$$

where the superscript signs indicate negative or positive *z*.

The antisymmetric part has no current on the pusher plate, there being no discontinuity in the rail current. In this case we have

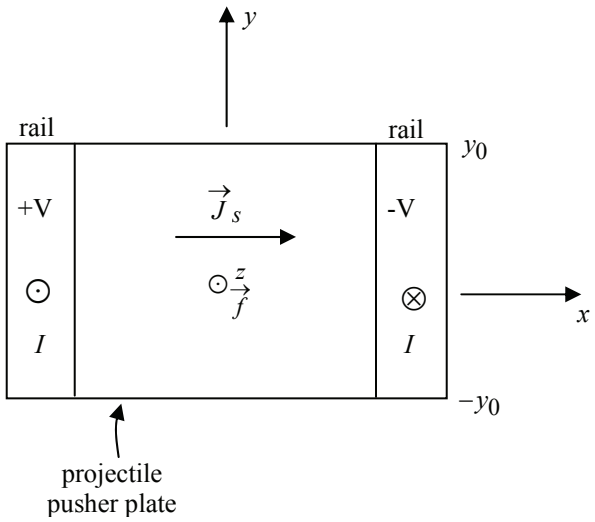

A. End View

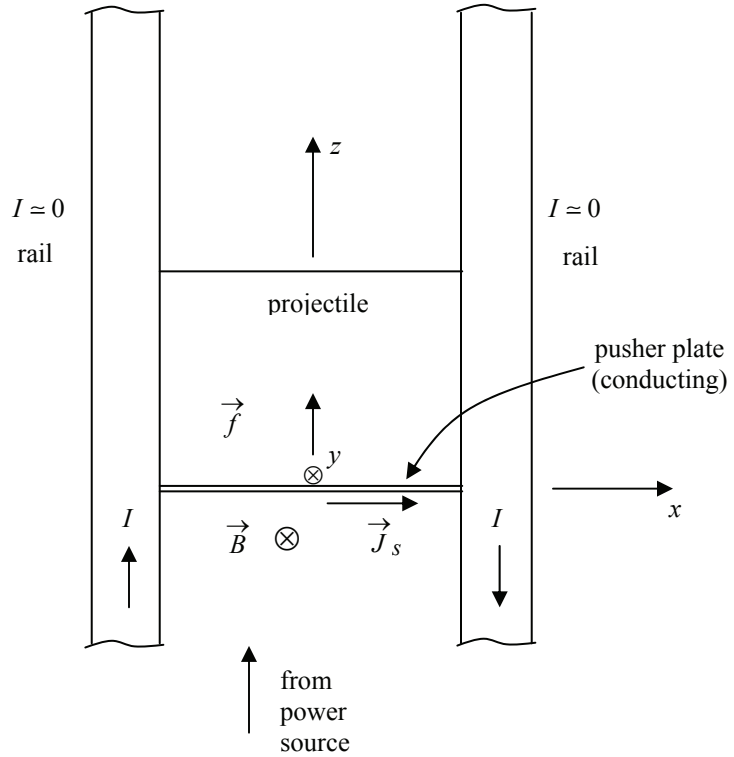

B. Bottom View

Fig. 2.1 Basic Railgun

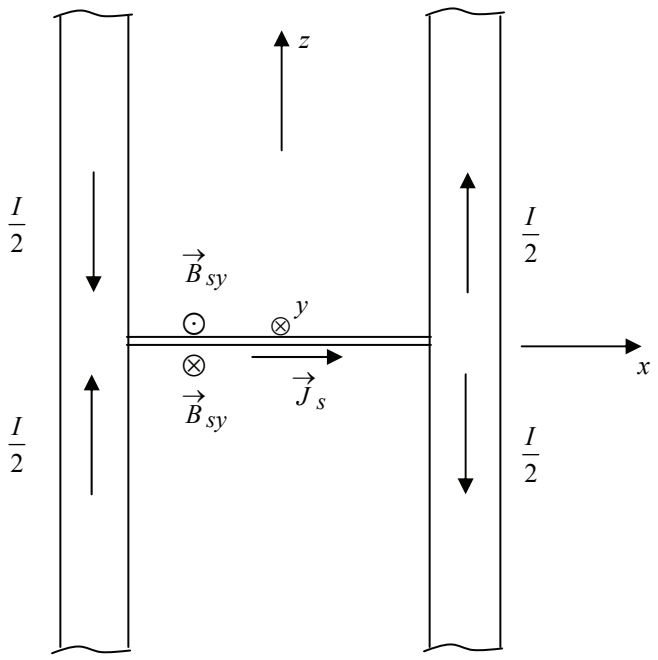

A. Symmetric part

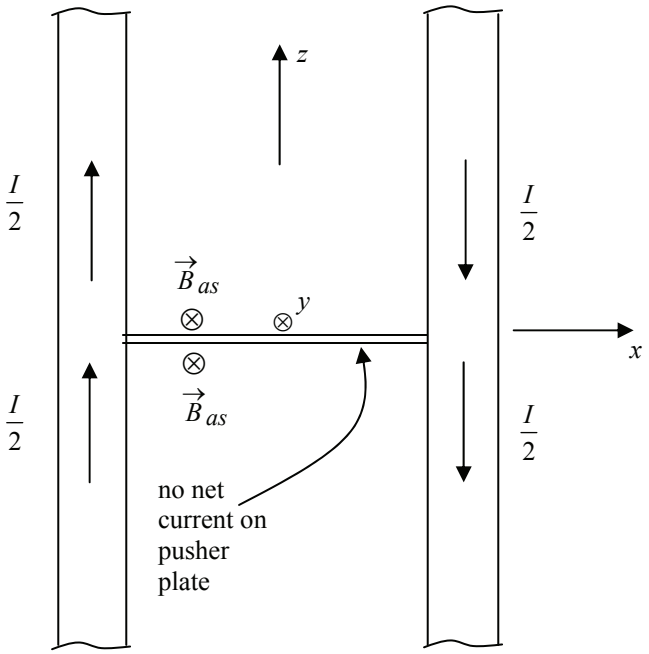

B. Antisymmetric part

Fig. 2.2 Magnetic-Field Configuration

$$\vec{B}_{as}^{(-)} = \vec{B}_{as}^{(+)} \tag{2.5}$$

Summing these two components the configuration in Fig. 2.1 is achieved. The discontinuity in the magnetic field across the pusher plate is

$$\Delta\vec{B} = \vec{B}^{(-)} - \vec{B}^{(+)} = \vec{B}_{sy}^{(-)} - \vec{B}_{sy}^{(+)} = 2\vec{B}_{sy}^{(-)} = \frac{\mu_0 I}{2y_0}\vec{1}_y \tag{2.6}$$

The pressure on the plate is then

$$\vec{f} = \vec{J}_s \times \Delta\vec{B} = \mu_0\left[\frac{I}{2y_0}\right]^2\vec{1}_z \tag{2.7}$$

This is a somewhat simplified view of the rail launcher. There is the general problem of enforcing the uniformity of $\vec{J}_s$ in the presence of the inductive effects of a time-changing magnetic field. (Current density tends to build up near edges of conductors.) Note that in general the surface current density on the rails is nonuniform, and this is ideally forced onto a uniform $\vec{J}_s$ on the pusher plate.

Nevertheless, this indicates that a large current can produce a large pressure, noting the quadratic dependence of the pressure on the current. Of course, there are similarly large forces on the rails, pushing them apart. These need to be opposed by appropriate mechanical structures.

3. Ideal Railgun Geometry

Pursuing symmetry concepts further, we can have a geometry based on a circular cylinder giving C_{2a} symmetry as indicated in Fig. 3.1.

In this case we have a pusher plate (disk) of radius a. This is in contact with a distributed set of rails (all parallel to the z axis). The rail currents are controlled to have a distribution in cylindrical coordinates (Ψ, ϕ, z) with

$$x = \Psi\cos(\phi) \ , \quad y = \Psi\sin(\phi) \tag{3.1}$$

as a sheet current (for negative z only)

$$\vec{J}_s^{(r)}(\phi) = -J_{s_0}\cos(\phi)\,\vec{1}_z \tag{3.2}$$

This matches a uniform sheet current in the pusher plate as

$$\vec{J}_s = J_{s_0}\,\vec{1}_x = J_{s_0}\left[\cos(\phi)\,\vec{1}_\Psi - \sin(\phi)\,\vec{1}_\phi\right] \tag{3.3}$$

giving a total current

$$I = 2aJ_{s_0} = -\int_{-\pi/2}^{\pi/2} \vec{J}_s^{(r)}(\phi) \cdot \vec{1}_z \; a\,d\phi \tag{3.4}$$

The analysis of the previous section still applies (y_0 now replaced by a). However, now the symmetry allows one to expand the fields in cylindrical coordinates only involving $\cos(\phi)$ and $\sin(\phi)$ terms, without higher order $(n\phi)$ terms, thereby simplifying the analysis. For quasistatic fields one has exponential dependence on z, and Bessel-function dependence on Ψ [6]. On the $z = 0$ plane in solving for the symmetric part of the fields, the tangential components of $\vec{B}$ are zero for $\Psi > a$, but discontinuous as in (2.4) for $\Psi < a$. The normal components are zero an $z = 0$ (again by symmetry). Fortunately for our problem the magnetic fields are much simpler on (and near) the $z = 0$ plane.

While this geometry gives a high degree of symmetry to the fields and avoids some of the problems associated with edges to achieve a uniform pressure, it has various practical implementation problems. Such a

distribution of $\vec{J}_S^{(r)}(\phi)$ can be approximately realized by a set of conductors, each carrying an appropriate current. However, such a configuration introduces significant complexity in producing all the various currents required. There are also the various mutual inductances to be considered.

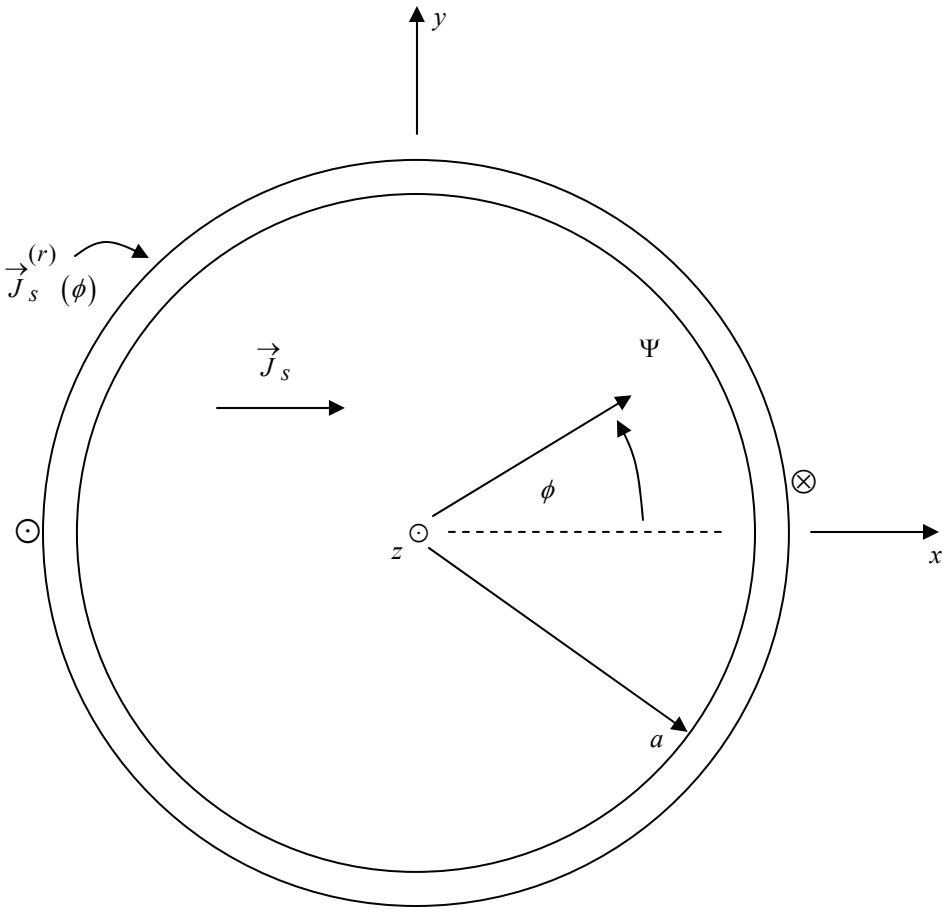

Rail currents are for negative *z*.

Fig. 3.1 Circular Cylindrical Geometry

4. Approximation By Deviation From the Ideal Case

From the previous section one can try to vary the rail geometry to obtain a more uniform sheet current on a circular-disk pusher plate. Two special cases are indicated in Fig. 4.1.

A first case in Fig. 4.1A has the curved rails each subtending an angle of 90°. As discussed in [2] the current density (and field) near the z axis is optimally uniform for this case of two conductors. In addition the $x = 0$ and $y = 0$ planes are symmetry planes. However, the current density near the rail edges has intensifications (singularities).

A second case in Fig. 4.1B has four rails, each carrying current $I/2$, as illustrated in Fig. 4.1B. Now the optimum angles for field uniformity are based on $\pm 30°$ away from the x axis as discussed in [1].

These two cases are examples of rail geometries which attempt to approximately realize the configuration in Fig. 3.1.

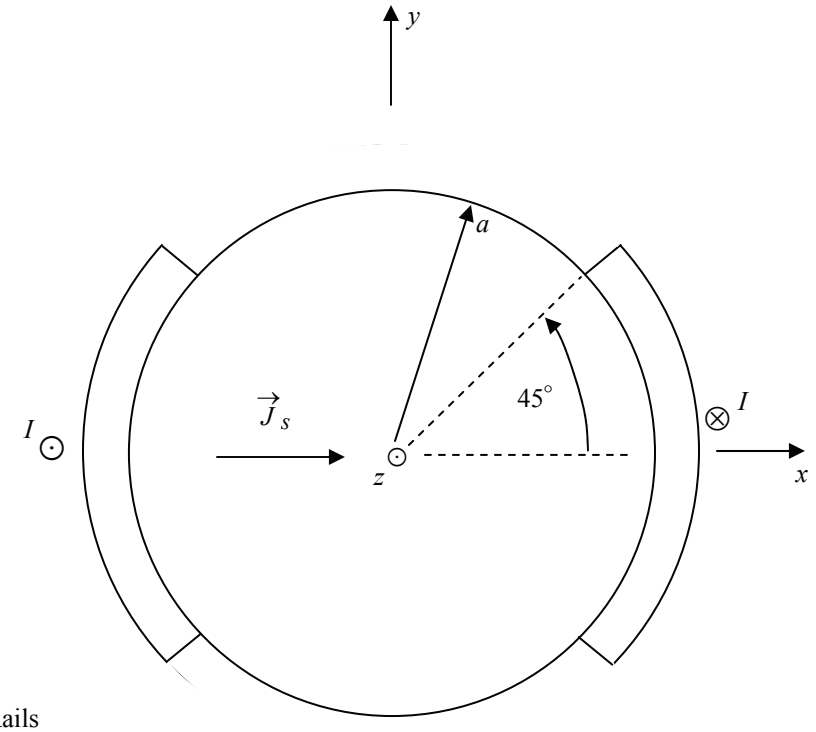

A. Two Curved Rails

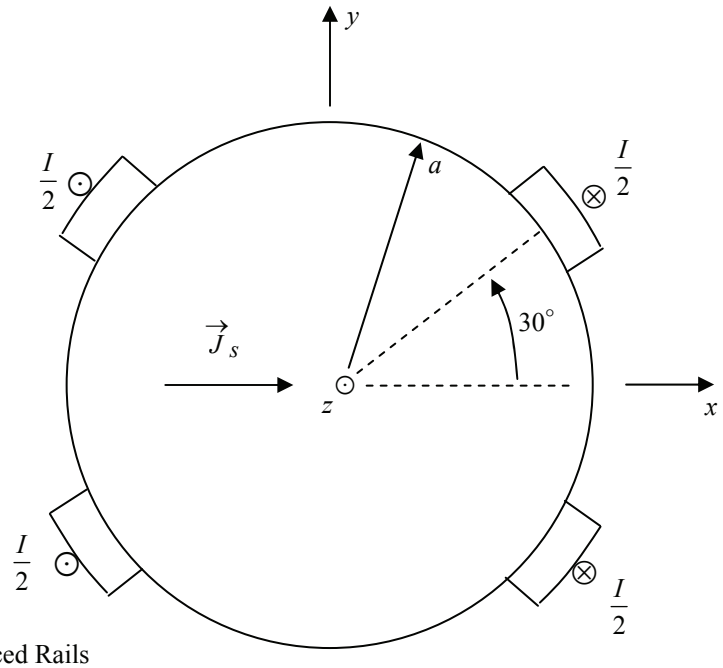

B. Four Optimally Placed Rails

Fig. 4.1 Some Alternate Rail and Projectile Geometries

5. Variation of Mass Density

As we have seen the pusher plate may have a nonuniform magnetic pressure. This in turn means that the projectile may be subjected to a nonuniform force distribution across its backside. This then tries to accelerate different parts of the projectile at different rates, potentially distorting the projectile.

One can compensate for this nonuniform pressure by varying the mass density of the projectile, at least near the pusher plate. Thus one may make the acceleration of the pusher plate more uniform across its surface.

6. Helical Railgun

By analogy with the usual rifle driven by exploding gas pressure, one can use rifling in an electromagnetic launcher. This can take the form of a helical railgun as illustrated in Fig. 6.1.

The basic idea is to even out the $\vec{J}_S \times \vec{B}$ forces by rotating the position of the launcher rails in contact with the projectile as the projectile moves along the circular cylindrical gun barrel. This, of course, assumes a circular cylindrical projectile, such as illustrated in Fig. 4.1. As the projectile passes along the gun barrel the $\vec{J}_S$ pattern on the pusher plate rotates. Portions of large force become positions of small force, and conversely. This makes the average forces over the projectile more uniform over time. One can define some $\phi_r(z)$ as a reference angle for the rails. This can increase or decrease, or even occasionally reverse direction, as the projective progresses along the gun barrel.

Note the forces F on the rails. Two parallel rails (as in previous sections) have these forces pushing the rails apart at all positions behind the projectile. As indicated in Fig. 6.1, as one progresses along the barrel the forces on a particular rail push the rail outward. Say we start where a rail is pushed to the left, then at a half rotation period along the barrel the same rail is pushed to the right (and so on). The rail itself then opposes the magnetic forces attempting to move it. The rail strengths are important to hold the rails in place, with significantly reduced sideway squeezing force required.

Another aspect of the helical rail configuration, concerns the external magnetic field. Parallel rails act like a line magnetic dipole, for which the external magnetic field falls off proportional to Ψ^{-2}. The helical configuration has alternating (reversing) direction of the magnetic moment as one progresses along the gun barrel. This results in a more rapid falloff of the external magnetic field.

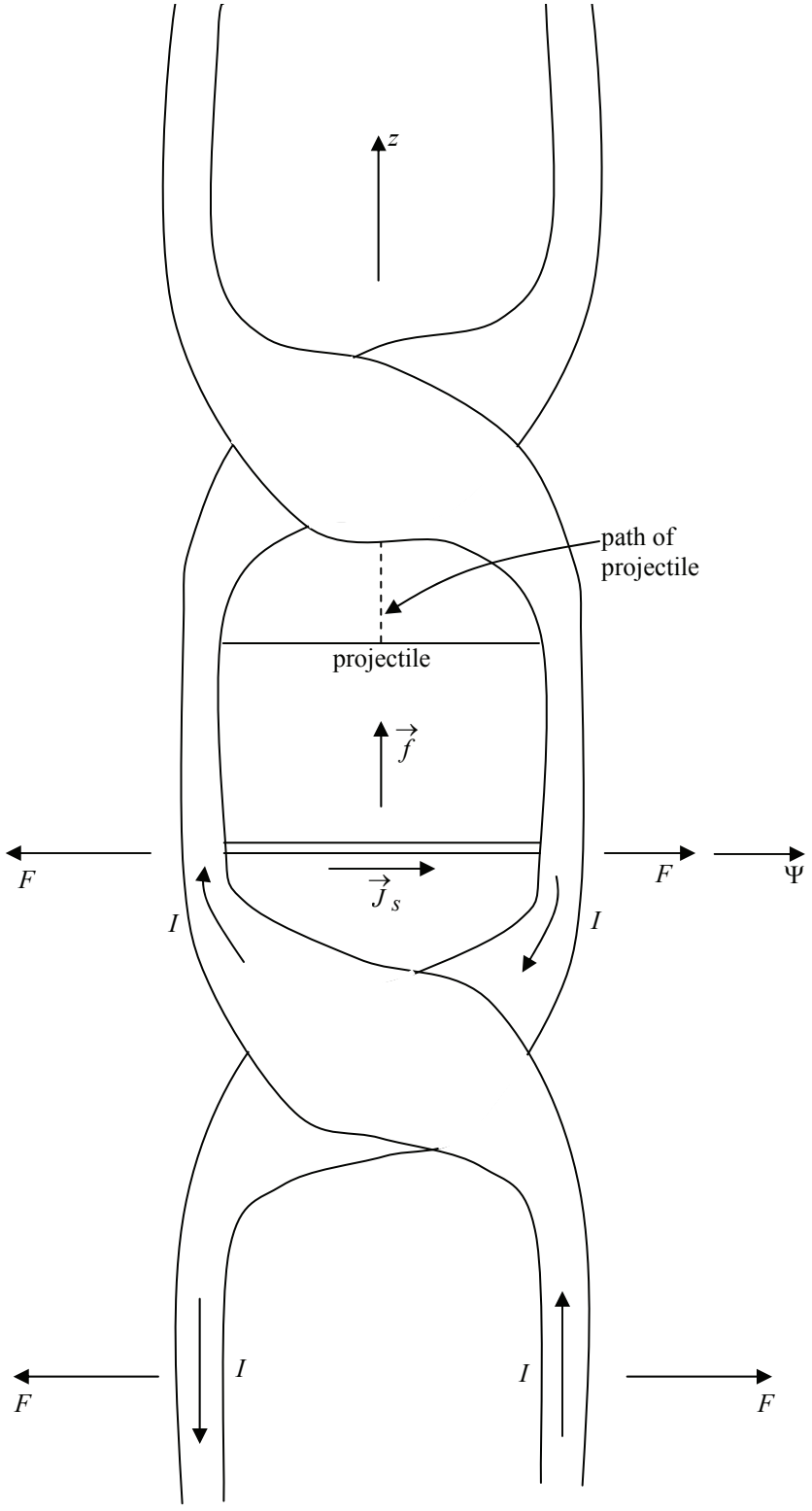

Fig. 6.1 Helical Railgun

7. Concluding Remarks

We now have many examples of concepts giving variations on the railgun theme. Each has its advantages and disadvantages. The future will tell the potential utility of such design concepts.

References

1. C. E. Baum, "Impedances and Field Distributions for Symmetrical Two Wire and Four Wire Transmission Line Simulators", Sensor and Simulation Note 27, October 1966.

2. T. K. Liu, "Impedances and Field Distributions of Curved Parallel-Plate Transmission-Line Simulators", Sensor and Simulation Note 170, February 1973.

3. J. H. Beno and W. F. Weldon, "Railgun Current Guard Plates: Active Current Management and Augmentation", IEEE Trans. Plasma Science, pp. 422-428, 1989.

4. D. Pavlik, R. Girgis, J. Repp, and D. Deis, "Investigations of the Electromagnetic Performance of Alternate Electromagnetic Barrel Designs", Proc. 8th IEEE Int'l. Pulsed Power Conf., pp. 754-759, 1991.

5. I. Kohlbert, A. Zielinski, and C. D. Lee, "Transient Electromagnetic Fields Produced by Pulsed Moving Conductors", ARL-TR-1931, April 1999.

6. R. V. Langmuir, *Electromagnetic Fields and Waves*, McGraw Hill, 1961.

7. C. E. Baum and H. N. Kritikos, "Symmetry in Electromagnetics", ch. 1, pp. 1-90, in C. E. Baum and H. N. Kritikos (eds.), *Electromagnetic Symmetry*, Taylor & Francis, 1995.